# Fault diagnosis for fuel cell systems: A data-driven approach using high-precise voltage sensors

Zhongliang Li [a, b, c, *], Rachid Outbib [a], Stefan Giurgea [b, c], Daniel Hissel [b, c], Alain Giraud [d], Pascal Couderc [e]

[a] Aix Marseille Univ, Université de Toulon, CNRS, LIS, Marseille, France
[b] FCLAB (Fuel Cell Lab) Research Federation, FR CNRS 3539, rue Thierry Mieg, 90010, Belfort Cedex France
[c] FEMTO-ST (UMR CNRS 6174), ENERGY Department, UFC/UTBM/ENSMM, France
[d] CEA/LIST, 91191 Gif-sur-Yvette Cedex, France
[e] 3D PLUS, 78532 BUC, France

## ARTICLE INFO

## ABSTRACT

Reliability and durability are two key hurdles that prevent the widespread use of fuel cell technology. Fault diagnosis, especially online fault diagnosis, has been considered as one of the crucial techniques to break through these two bottlenecks. Although a large number of works dedicated fuel cell diagnosis have been published, the criteria of diagnosis, especially online diagnosis have not yet been clarified. In this study, we firstly propose the criteria used for evaluating a diagnosis strategy. Based on that, we experimentally demonstrate an online fault diagnosis strategy designed for Proton Exchange Membrane Fuel Cell (PEMFC) systems. The diagnosis approach is designed based on advanced feature extraction and pattern classification techniques, and realized by processing individual fuel cell voltage signals. We also develop a highly integrated electronic chip with multiplexing and high-speed computing capabilities to fulfill the precise measurement of multi-channel signals. Furthermore, we accomplish the diagnosis algorithm in real-time. The excellent performance in both diagnosis accuracy and speediness over multiple fuel cell systems is verified. The proposed strategy is promising to be utilized in various fuel cell systems and promote the commercialization of fuel cell technology.

© 2018 Elsevier Ltd. All rights reserved.

## 1. Introduction

Fuel cell technology, because of its potential for effectively alleviating environmental and resource issues, has been attracting considerable increasing attention. Among the various fuel cells, proton exchange membrane fuel cell (PEMFC), thanks to its high power density and efficiency, low operating temperature, and quick response to load, is the most promising one to be widely applied in both stationary and automotive cases. However, reliability and durability are currently two main barriers which prevent the process for its wide applications [1,2]. Among the solutions, fault diagnosis, more particularly online diagnosis, dedicated to

detecting, isolating, and analyzing different faults, has proved to be beneficial for keeping fuel cell systems operating safely, reducing downtime and mitigating performance degradation [3—5].

The operation of a PEMFC system involves multiple auxiliary subsystems other than fuel cell stack, and requires multi-field knowledge, for example complex electrochemistry, thermodynamics, and fluid mechanics. To accurately detect and identify the faults occurring in the system is not a trivial task. During the last decade, considerable attention has been focused on the topics related to fault diagnosis for PEMFC systems.

Among the most substantial approaches, model based fault diagnosis approaches have been proposed. A review of model based methods is available in Ref. [6]. Most of these approaches are based on some general input-output or state space models, which are usually developed from the physical and mathematical knowledge of the process [7]. In Ref. [8], the authors developed an electrical equivalent circuit which can be seen as an analytical model of the concerned PEMFC system. The component parameters are identified and the variation of the specific electrical component values

* Corresponding author. Aix Marseille Univ, Université de Toulon, CNRS, LIS, Marseille, France.
*E-mail addresses:* zhongliang.li@lis-lab.fr (Z. Li), rachid.outbib@lsis.org (R. Outbib), stefan.giurgea@utbm.fr (S. Giurgea), daniel.hissel@univ-fcomte.fr (D. Hissel), alain.giraud@cea.fr (A. Giraud), pcouderc@3d-plus.com (P. Couderc).

can be seen as the indicator of the corresponding faults. In Ref. [9], a linear parameter varying (LPV) model is built for a commercial PEMFC system. An observer is proposed based on the proposed LPV model. Then, the residuals can be computed by comparing the process outputs and the outputs estimated from the observer. The similar methods are also used in Refs. [10,11]. Besides designing a specific observer, the parity relation is also used for residual generation procedure in a more straightforward way [12]. To carry out the above mentioned three kinds of analytical model based approaches, an accurate process model of PEMFC systems is necessary. However, modeling the PEMFC systems is a rather difficult task. Especially, the identification of fuel cell inner parameters concerning the operation, the geometries as well as the materials is difficult [13]. Even the parameters are identified, some of them are time-varying because of the ageing degradation. In addition, the existing models are usually not able to fulfill sufficient accuracy, generalization and real-time implementability, which makes model based approaches insufficiently suitable for wide practical applications [14].

Another branch named data-driven diagnosis has been gaining increasing attention. The data-driven methods are those make use of the information from the historical data other than an analytical model. A review of data-driven methods is available in Ref. [4]. In Refs. [15,16], and [17], fuzzy inference and neural networks are used to build "black-box" models whose parameters are obtained by fitting the experimental data obtained in fault free state. With these "black-box" models, the diagnosis can be realized by evaluating the difference between the real system outputs and the model outputs. In Ref. [18], a multivariate analysis technique, named principal component analysis (PCA), is used for diagnosis by analyzing the variables measured by multiple sensors installed in a PEMFC system. In Ref. [19], the fuzzy clustering method is used to process the signals acquired from a commercial PEMFC system in order to achieve fault diagnosis. In Refs. [20] and [21], Bayesian networks classification is used for the PEMFC diagnosis. In Refs. [22,23], and [24], the signal processing methods, fast fourier transform, wavelet transformation, multifractal formalism, are respectively used to extract the features which are sensitive to faults from the fuel cell stack voltage signals. Although some interesting preliminary results have been proposed in the frame of data-driven diagnosis, the online validation of those approaches in different real PEMFC systems has not yet been announced.

Actually, some criteria have to be satisfied to realize online diagnosis for PEMFC systems serving in real conditions. First, the sensors for measuring the variables serving as the inputs of the fault diagnosis approach should be minimized and arranged in limited space. The intrusive and/or costly sensors or instruments should be avoided whenever possible. Second, the diagnosis accuracy should be maintained at a high level with respect to different faults and different PEMFC systems. Third, the online diagnosis approach needs to be computationally efficient since it is usually implemented in some "on-board" embedded system with limited computational power available [25,26]. Fourth, because of ageing effects, fuel cells' behaviors are time-variant. The diagnosis approach should be capable of being adapted online. In addition, the serial-connected single fuel cells which compose a fuel cell stack are usually considered to be identical in the existing approaches. Nevertheless, the inhomogeneity among cells should be more emphasized when we talk about "faults". This is because usually a proportion of fuel cells fall into faulty state first when a fault occurs [27,28].

In this article, we propose and experimentally demonstrate an online fault diagnosis strategy for PEMFC systems. To achieve the diagnosis goal, we designed an reduced volume application specific integrates circuit (ASIC) which integrate multichannel voltage sensors of giant magneto resistance (GMR) type, and a field programmable gate array (FPGA) based computing unit [29,30]. The individual fuel cell voltages can be precisely measured and treated as the input variables of the diagnosis approach. The discriminant features are extracted using fisher discriminative analysis (FDA) from the vectors composed by cell voltages and classified the features using support vector machine (SVM) into different classes that represent different states of health. Besides the requirements for a basic diagnosis approach, the novel fault detection and online adaptation functions are also developed and added to the proposed approach. They are realized through using specifically designed diagnosis rules and an incremental learning method. We verified the efficiency of our strategy via the experiments on several stacks and multiple faulty types. To our knowledge, this work is the first to provide a high-performance online diagnosis strategy implemented in an ASIC for PEMFC systems.

The rest of the paper is organized as follows: the development process of the proposed diagnosis strategy is given in Section 2. Section 3 and Section 4 present respectively the diagnosis approach and the ASIC designed to realize diagnosis function. Experimental platform and database preparation are described in Section 5. Diagnosis results are summarized and analyzed in Section 6. We finally conclude the work in Section 7.

## 2. Diagnosis strategy development process

The proposed data-driven diagnosis strategy consists of offline and online stages (see Fig. 1(a)). The feature extraction (FDA) and the classification models (SVM) are trained and tested offline. The objective of the test stage is to optimize the parameters used for SVM. The trained models are implemented online to achieve the diagnosis goal. Moreover, based on the data sampled online, the SVM model can be adapted online.

The realization process is shown in Fig. 1(b). In the offline stage, the historical data (individual cell voltages) are measured using the GMR sensors integrated in the ASIC and saved as the training and test database into a PC. Then the diagnosis model is trained using the PC and programmed into the memory of the ASIC. In the online stage, the variables (individual cell voltages) are measured and processed using the ASIC with the model trained offline.

## 3. Diagnosis approach

In this section, the diagnosis problem and the involved methodologies are presented mathematically in a general manner. Actually, the main focus of this paper is to provide the completed implementation process of the proposed diagnosis strategy, which includes both software and hardware developments. The mathematical details of the involved algorithms are provided by citing several published works.

### 3.1. Problem formulation

The diagnosis approach proposed in this study belongs to the category of supervised methods. The basic tasks of fault diagnosis, i.e. fault detection and isolation, can be abstracted as a typical pattern classification problem (see Fig. 2).

Suppose that the fuel cell stack in a concerned system is composed of $M$ single fuel cells. At a certain time, the individual cell voltages are measured and denoted as a vector $\boldsymbol{v} = [v_1, v, ..., v_M]^T$. Suppose that we have a training dataset $\boldsymbol{V}$ which consists of $N$ such vectors, i.e. $\boldsymbol{V} = \{\boldsymbol{v}_1, \boldsymbol{v}_2, ..., \boldsymbol{v}_N\}$. These vectors are known to be distributed in the classes denoted as $\Omega_0, \Omega_1, \Omega_2, ..., \Omega_C$, in which the class label 0 corresponds to the fault free state, while 1, 2, ..., $C$ correspond to the faults of various types. The class label $g_i$ of vector
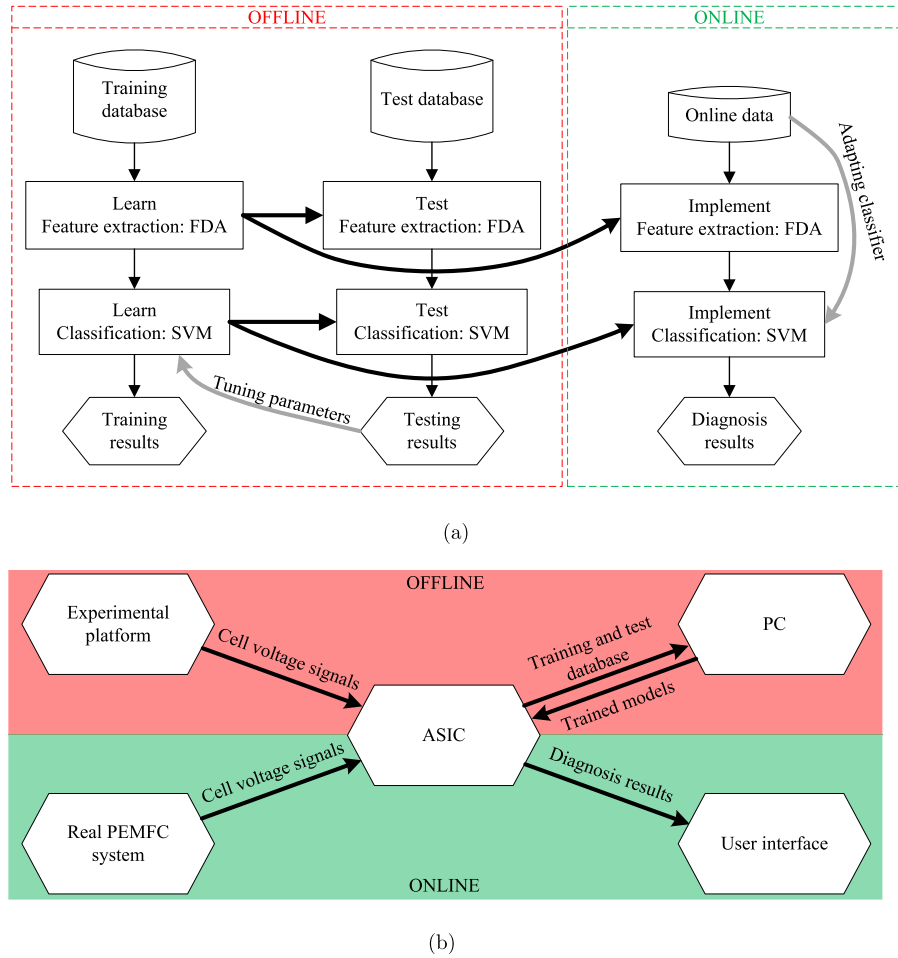
(a)



(b)

**Fig. 1.** Diagram of the proposed diagnosis approach and of the realization process. (a) Workflow of the proposed diagnosis approach. (b) Realization process of the diagnosis strategy.

$\boldsymbol{v}_i$ is known in prior. Based on the dataset $\boldsymbol{V}$, a function denoted as $F(\cdot)$ can be trained offline. Through the function, the class label of a given vector formed by the cell voltages can be determined as

$$g_n = F(\boldsymbol{v}_n) \tag{1}$$

The diagnosis procedure is the process of implementing this function online.

A large dimensional number $M$, i.e. the single fuel cell number, may cause a heavy burden of online computation and a reduced diagnosis power. We therefore propose a two-step diagnosis procedure to solve the problem as follows: a feature extraction stage to reduce the original data dimensional number is carried out first, as

$$\boldsymbol{z}_n = f_1(\boldsymbol{v}_n) \tag{2}$$

where $\boldsymbol{z}_n$ is a $L$-dimensional vector composed of features ($L < M$). Then, the classification is implemented in the feature space as

$$g_n = f_2(\boldsymbol{z}_n) \tag{3}$$

Such that the diagnosis procedure is transformed into a two-step procedure. By comparing several representative feature extraction and classification methods from the point of view of diagnosis precision and computational complexity, FDA and SVM methods were selected as the feature extraction and classification tools, respectively [31].

### 3.2. Principle of FDA

FDA is a supervised technique developed to extract the features from the data in the hope of obtaining a more manageable classi-fication problem [32]. The objective of FDA is to project the data into a lower dimensional space in which the variance between classes is maximized while the variance within an identical class is minimized. Through the training process, $C$ projecting vectors ($C$ fault types in the training dataset), denoted as $\boldsymbol{w}_1, \boldsymbol{w}_2, \dots \boldsymbol{w}_C$, can be determined in the offline training phase. The features of the vector $\boldsymbol{v}_n$ can be computed as $\boldsymbol{z}_n = [\boldsymbol{w}_1^T \boldsymbol{v}_n, \boldsymbol{w}_2^T \boldsymbol{v}_n, \dots, \boldsymbol{w}_C^T \boldsymbol{v}_n]^T$. The details on FDA implementation can be found in Ref. [31].

### 3.3. Principle of SVM

SVM is a classification method developed originally by V. Vapnik in 1998 and has been considered as the present state of art classifier [33]. SVM functions by projecting the data into a high-dimensional space and constructing a hyperplane which separates the cases of different classes in this space. Different from the basic SVM, spherical shaped multi-class support vector machine (SSM-SVM), considered as a modified version, was employed in our approach [34]. The principle of SSM-SVM is to project the original data into a high-dimensional space and seek multiple class-specific spheres which enclose the samples from an identical class while excluding those from the other classes in this space (see Fig. 3). The projection
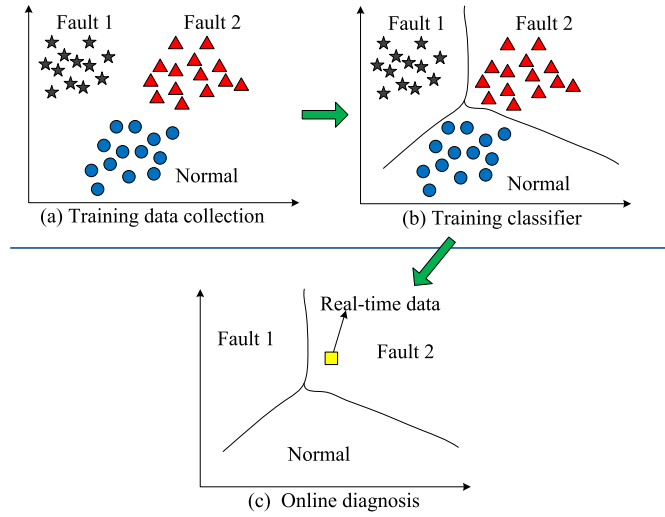
**Fig. 2.** Principle of classification based fault diagnosis. The implementation of the approach can be divided into three steps. (a) The historical data in both health state and concerned faulty states are collected as the training data base. In this case, the data are distributed in three classes: normal, fault 1 and fault 2. (b) A classifier is trained based on the training data base. The trained classifier is described as the boundaries among the classes. (c) The trained classifier is performed online. According to the classifier or the boundaries here, an arbitrary online sample is classified into one of the concerned classes. Fault detection and isolation is thus realized. In this case, the online sample is classified into fault 2 class.

from original space to high-dimensional space and some data processing are realized by introducing a kernel function and playing "kernel trick". Training a SVM classifier can be finally abstracted as a quadric problem, while implementing a SVM classifier involves a small proportion of the training data which are named "support vectors".

To determine the class label of a sample $\boldsymbol{z}_n$, the following criterion is used

$$g_n = \underset{i}{\arg\max} G_i(d_i(\boldsymbol{z}_n)) \quad i = 0, 1, 2, \ldots, C \tag{4}$$

where $G_i$ is a smooth monotonous decreasing function, $d_i(\boldsymbol{z}_n)$ is the distance from $\boldsymbol{z}_n$ to the $i$th sphere center and it can be calculated based on training result. See Ref. [14] for more details of SSM-SVM classification.

### 3.4. Diagnosis rules

A conventional classification method can only classify a sample into a known class. It will lose its efficiency as a sample comes from a novel class, i.e. a novel faulty mode in our case. In order to recognize the novel faulty mode, we propose to set boundaries for the spheres in high-dimension space. The samples from a novel cluster can thus be detected if they are outside all the closed boundaries. To realize this, the function $G_i$ in terms of $d_i(\boldsymbol{z})$ is defined as

$$G_i(d_i(\boldsymbol{z})) = \begin{cases} 0.5\left(\dfrac{1 - d_i(\boldsymbol{z})/R_i}{1 + \zeta_1 d_i(\boldsymbol{z})/R_i}\right) + 0.5 & \text{if } d_i(\boldsymbol{z}) \leq R_i \\ 0.5\left(\dfrac{1}{1 + \zeta_2(d_i(\boldsymbol{z}) - R_i)}\right) & \text{otherwise} \end{cases} \tag{5}$$

where $R_i$ is the radius of $i$th sphere, $\zeta_1$ and $\zeta_2$ are constants that satisfy $R_i\zeta_2(1 + \zeta_1) = 1$. It could be proved that $G_i : \mathbb{R}_+ \to \mathbb{R}_+$ is a smooth decreasing function with $\lim\limits_{\tau \to \infty} G_i(\tau) = 0$.

It is considered that a sample $\boldsymbol{z}$ belongs more probably to the class with the shortest distance from the sphere center to the
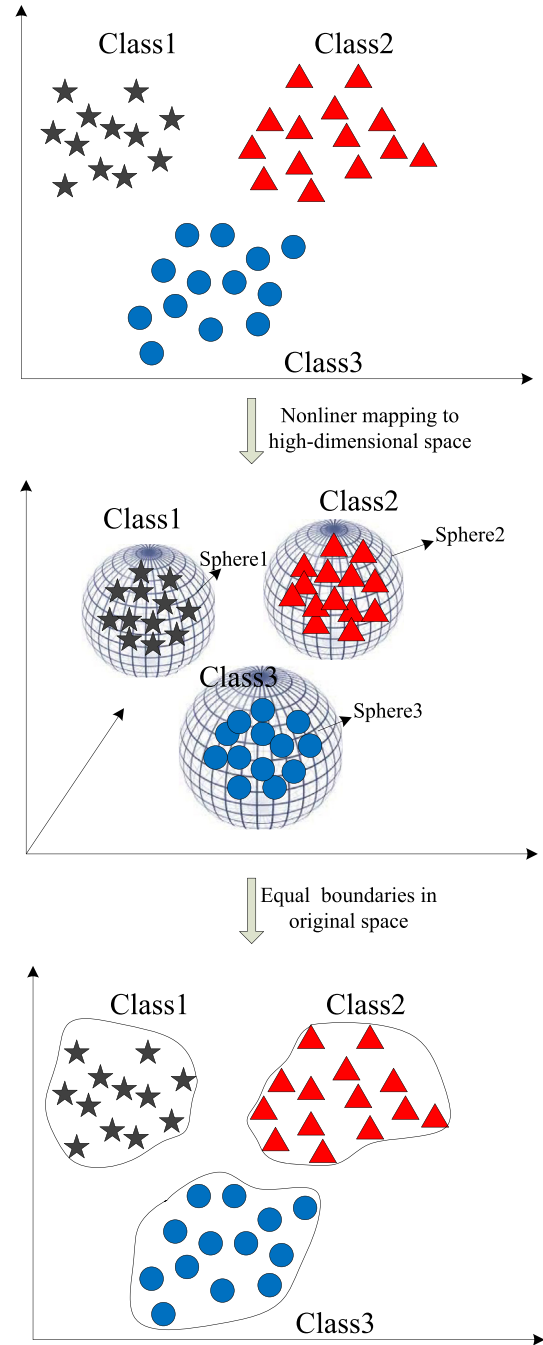


**Fig. 3.** Principle of SSM-SVM classification. The training data are distributed in three classes labeled by class 1, class 2 and class 3. Through nonlinear mapping, the original data are projected into high-dimensional space (3-dimension in this case). In the high-dimensional space, the class-specific spheres can be found through training. The class-specific spheres enclose the samples from a specific class, while excluding those from the other classes. These spheres can be seen as the class-specific boundaries in the original space.

sample. However, if this distance is still larger than a threshold, we will consider the sample is from a novel class (novel fault mode). Mathematically, the diagnosis rule is

$$g_n = \begin{cases} \underset{i}{\arg\max} G_i(d_i(\boldsymbol{z})) & \text{if } \max G_i(d_i(\boldsymbol{z})) \geq \delta_i \\ \text{new} & \text{if } \max G_i(d_i(\boldsymbol{z})) < \delta_i \end{cases} \tag{6}$$

where the threshold $\delta_i$ is determined based on a calibration dataset

with $N_i$ elements, and a way to fix its value is to use the *3-sigma law*:

$$\delta_i = M_i - 3\sqrt{\frac{1}{N_i}\sum_{g_n=i}(G_i(d_i(\mathbf{z})) - M_i)^2} \qquad (7)$$

with $M_i = \frac{1}{N_i}\sum_{g_n=i} G_i(d_i(\mathbf{z}_n))$.

### 3.5. Online adaptation method

Traditional SVM training is performed in one data batch and it must be redone from scratch if the training dataset varies. The computational cost for the training procedure is usually heavy and realized offline. To realize online updating of the classifier as time goes on, we propose here an incremental learning method for training the proposed SSM-SVM [14]. In this method, the solution for $N + 1$ training data could be formulated in terms of the solution for $N$ data and one new data point. The light computational complexity makes the incremental learning procedure suitable for online use. The theoretical deduction of incremental learning can be found in Ref. [14].

## 4. ASIC developed for implementing the diagnosis approach

Since the input variables for the diagnosis approach we propose are individual cell voltages, a sensor capable of precisely measuring the voltage signals of low amplitude and multiplexing is required. We propose here an integrated voltage sensor which is based on GMR technology [29]. Compared with the traditional Hall effect sensors which are commonly used for voltage or current measurement, the GMR sensors exhibit a much higher sensitivity especially in low current (voltage), high precision applications [35]. Knowing that a single cell voltage is usually less than 1 V, GMR sensors are well suited in our case. Moreover, the sensor developed here also improves the present state of the art in the aspects of increasing insulation capability ($> 2000kV$) [36].

To implement the proposed diagnosis approach, multiple GMR voltage sensors are packaged with a commercial system on chip (SoC) FPGA device which functions as the computation and communication unit. As shown in Fig. 4(a), these components are designed in the form of a 3D integration circuit. The upper layer taking charge of computation and communication can be seen as the "main board". In this layer, the Smartfusion on-chip system developed by Microsemi is integrated. The device integrates an FPGA fabric, an ARM Cortex-M3 Processor, and programmable analog circuitry. The ARM Cortex-M3 processor is an 100 MHz, 32-bit CPU. The programmable analog circuitry can function as the D/A and A/D conversion blocks. This integrated device is equipped with up to 512 KB flash and 64 KB of SRAM. Besides, another two 16 M memory chips is added to the system. With the abundant connecting ports, different kinds of communications can be realized with other devices. The other two layers, which are equipped with GMR sensors, are adapted for measuring multi-channel voltage signals precisely. The appearance of the 3D ASIC and the test board are shown respectively in Fig. 4(b) and (c).

## 5. Database preparation

In order to generate the database for training and testing the diagnosis model as well as validating the performance of online implementation, we carried out a series of experiments including the ones under normal operating condition and faulty conditions. The faults created deliberately cover the abnormal operations in different components of a PEMFC system, such as the water management
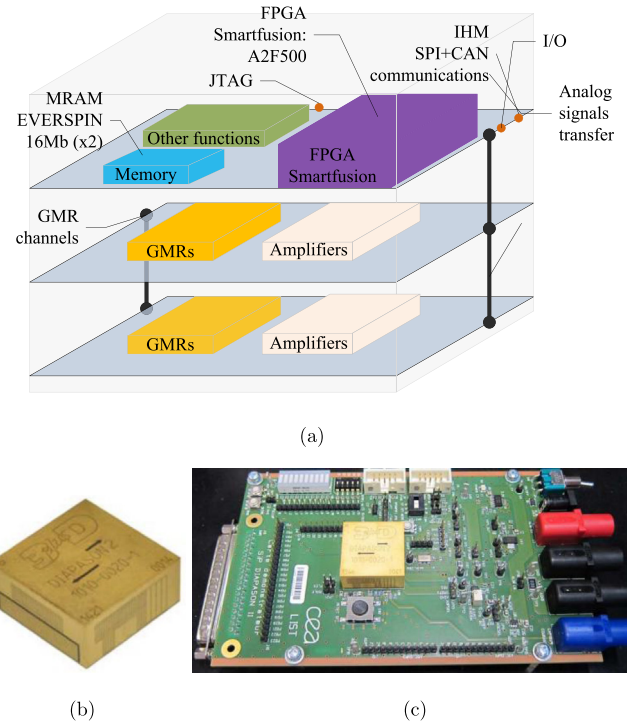


(a)



(b)                                                      (c)

**Fig. 4.** ASIC designed for monitoring individual fuel cell voltages and implementing the diagnosis approach. (a) The architecture of the ASIC, which was specially designed for the PEMFC system diagnosis. (b) The appearance of the designed ASIC. The ASIC is with compact package dimensions of $27 \times 27 \times 12mm^3$. (c) The ASIC is installed into a printed circuit board (PCB) which is equipped with the connectors, test points and LED lights.

subsystem, the temperature management subsystem, the electric circuit, the air and hydrogen circuits. The faults studied are usually considered as "reversible" or "recoverable", which means they can be corrected through appropriate operations and do not cause the permanent defects in the systems. Actually, accurate diagnosis of this kind of faults can usually avoid the occurrence of those so-called permanent faults. During the experiments the data were captured using the designed ASIC and saved into the disk of a PC.

### 5.1. PEMFC platform

A 1 kW and a 10 kW experimental platform, which had been developed in-lab, were employed to fulfill the experimental requirements (see Fig. 5). In the hydrogen and air circuits, the temperatures, pressures, flow rates, and relative humidifies can be regulated in a wide range. A thermal-regulated water circuit ensures the flexible control of the stack temperature. The load current profile can be defined or simulated with the help of a DC electronic load. A terminal is installed into the stack to facilitate the connection to the ASIC and to monitor the cell voltages.

The platform enables us to emulate different faults artificially, and thus generate the database for both offline training and online validation. In order to verify the generalization performance of the proposed approach, three stacks from different industrial suppliers and with different cell numbers, power levels, mechanical designs were explored respectively on the two platforms (Fig. 6, Table 1 and Table 2).

### 5.2. Concerned faults

Thanks to the home-made platforms in which a number of operating parameters can be set flexibly, we experimentally
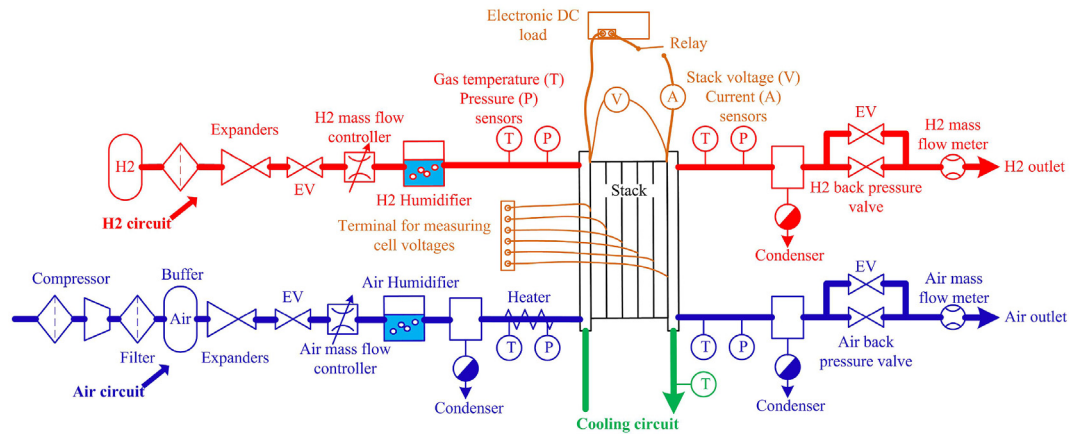
**Fig. 5.** Schematic of the platforms used for generating the training and test database and for online validation.



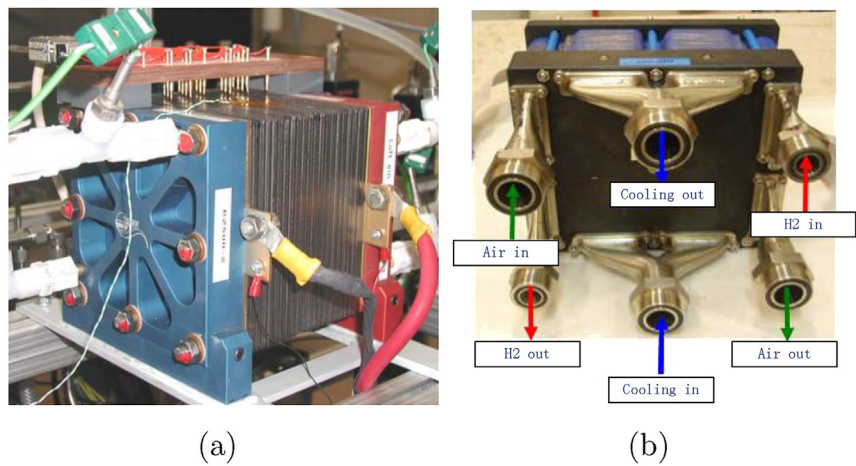(a)                                                                     (b)

**Fig. 6.** (a) 20-cell stack installed in the platform. (b) Appearance of the 8-cell stack and 40-cell stack.

simulated a variety of faults that can potentially occur in different components of a PEMFC system. In order to cover the possible fault types, 7 fault types involving different subsystems or components were explored in this study. These faults and corresponding operations are summarized in Table 3. In addition to the individual cell voltages, a detailed measurements of temperatures, current, pressures and gas flow rates have been achieved thanks to the well-equipped platforms. In this study, the importance is put on the combination of ASIC and data-driven diagnosis approach and their implementation for various fuel cell stacks. The detailed waveforms and analysis of the acquired data during each fault experiment have been summarized in the previous articles [37] [28] [38].

## 6. Results

We carried out a number of experiments in both normal operating and faulty cases to collect the data for training and testing the proposed diagnosis model. Then, the trained diagnosis model was programmed into the memory of the ASIC and implemented online.

As the individual cell voltages were used as the variables for diagnosis, the dimensional number of the original data was equal to

**Table 1**
Technical parameters of the 20-cell stack.

| Parameter | Value |
| --- | --- |
| Active area | 100 cm$^2$ |
| Flow field structure | serpentine |
| Electrode surface area | 100 cm$^2$ |
| Nominal output power | 500 W |
| Operating temperature region | 20–65 °C |
| Maximum operating pressures | 1.5 bar |
| Anode stoichiometry | 2 |
| Cathode stoichiometry | 4 |

**Table 2**
Technical parameters of the 8-cell stack and 40-cell stack.

| Parameter | Value |
| --- | --- |
| Active area | 200 cm$^2$ |
| Stoichiometry $H_2$ | 1.5 |
| Stoichiometry $Air$ | 2 |
| Pressure at $H_2$ inlet | 150 kPa |
| Pressure at $Air$ inlet | 150 kPa |
| Pressure differential between anode and cathode | 30 kPa |
| Temperature (exit of cooling circuit) | 80 °C |
| Anode relative humidity | 50% |
| Cathode relative humidity | 50% |
| Current | 110 A |
| Voltage per cell | 0.7 V |
| Electrical power of 8-cell stack | 616 W |
| Electrical power of 40-cell stack | 3080 W |

**Table 3**
Experiments on various health states carried out on different PEMFC stacks.

| Stack | Health state description | Location | Operation | Notation |
|---|---|---|---|---|
| 20-cell stack | Normal operating | Whole system | Nominal operation | Normal |
| | Flooding | Water management subsystem | Increase air relative humidity | $F_1$ |
| | Membrane drying | Water management subsystem | Deactivate air humidifier | $F_2$ |
| 8-cell stack | Normal operating | Whole system | Nominal operation | Normal |
| | High current pulse | Electric circuit | Short circuit | $F_3$ |
| | High temperature | Temperature subsystem | Stop cooling water | $F_4$ |
| | High air stoichiometry | Air supply subsystem | Increase air stoichiometry to 2.0 normal value | $F_5$ |
| | Low air stoichiometry | Air supply subsystem | Decrease air stoichiometry to 0.6 normal value | $F_6$ |
| | Anode CO poisoning | $H_2$ supply subsystem | Feed hydrogen with 10 ppm CO | $F_7$ |
| 40-cell stack | Normal operating | Whole system | Nominal operation | Normal |
| | High current pulse | Electric circuit | Short circuit | $F_3$ |
| | High temperature | Temperature subsystem | Stop cooling water | $F_4$ |
| | High air stoichiometry | Air supply subsystem | Increase air stoichiometry to 2.2 normal value | $F_5$ |
| | Low air stoichiometry | Air supply subsystem | Decrease air stoichiometry to 0.65 normal value | $F_6$ |

the cell number in the concerned stack. By using the FDA method, the features were extracted from the original data. A part of extracted features are shown in Fig. 7(a), Fig. 7(b) and (c). From these figures, it can be seen that the features in normal state and different faulty states are generally separated in the lower dimensional feature space. The characteristic lightens the computational burden and improves the performance of the classification following feature extraction step [37].

In a diagnosis cycle, classification is conducted in the feature space following the feature extraction procedure. SSM-SVM, combined with the diagnostic rule, is implemented in this phase. To construct the SSM-SVM classifier, the radial basis function (RBF)
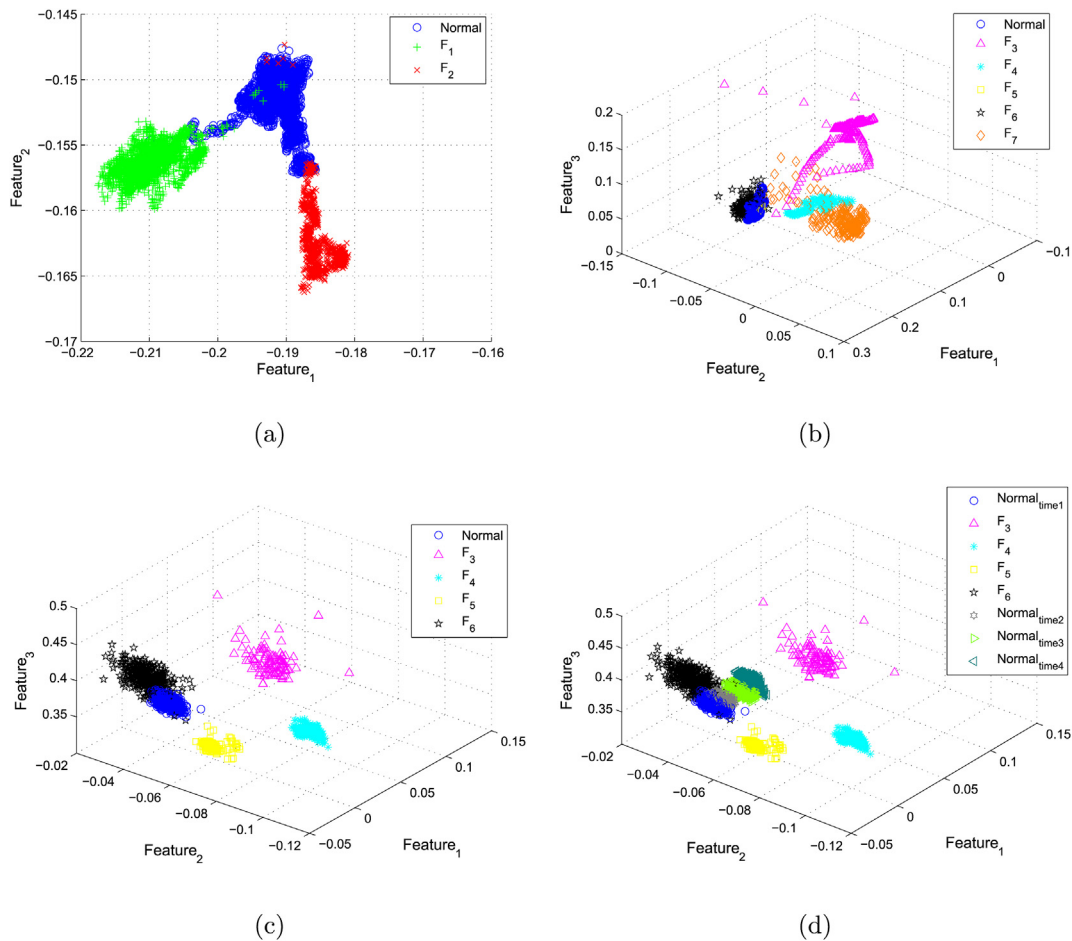


**Fig. 7.** Features extracted from data of cell voltages. Normal, $F_1$, $F_2$, $F_3$, $F_4$, $F_5$, $F_6$ and $F_7$ represent respectively the normal state, membrane drying fault, flooding fault, high current pulse fault, cooling water stopping fault, high air stoichiometry, low air stoichiometry, and anode CO poisoning. (a) 2-dimensional features extracted from the data in normal, $F_1$ and $F_2$ faulty states for a 20-cell stack. (b) 3-dimensional features extracted from normal and 5 various faulty states for a 8-cell stack. (c) 3-dimensional features extracted from normal and 4 various faulty states for a 40-cell stack. (d) 3-dimensional features extracted from normal state and 4 various faulty states for a 40-cell stack. The data in normal state (denoted as $Normal_{time1}$, $Normal_{time2}$, $Normal_{time3}$, $Normal_{time4}$) are sampled at different time points.

**Table 4**
Diagnosis accuracy for different faults for different PEMFC stacks.

| Fault | $F_1$ | $F_2$ | $F_3$ | $F_4$ | $F_5$ | $F_6$ | $F_7$ |
|---|---|---|---|---|---|---|---|
| Stack 1 (20-cell) | 94.01% | 99.21% | – | – | – | – | – |
| Stack 2 (8-cell) | – | – | 91.63% | 95.02% | 100.00% | 89.44% | 99.08% |
| Stack 3 (40-cell) | – | – | 93.55% | 100.00% | 99.56% | 85.14% | – |

$F_1$: Membrane drying fault; $F_2$: Flooding fault; $F_3$: High current pulse fault; $F_4$: Cooling water stopping fault; $F_5$: High air stoichiometry; $F_6$: Low air stoichiometry; $F_7$: Anode CO poisoning.

was selected as the "kernel function", and parameters including the penalty factor and kernel parameter were optimized based on the test database.

### 6.1. Diagnosis accuracy

We evaluated the online implementation results using two criteria: false alarm rate (FAR) which is the rate of the samples in normal state wrongly diagnosed into the faulty classes, and the diagnosis accuracy of each specific fault type. According to the recorded diagnosed results, FAR reaches respectively 2.82%, 0%, 2.09% for the three stacks, which exhibits a low level. The diagnosis accuracies of the 7 fault types concerned are listed in Table 4. It should be noted that the parameters are maintained at a high level ($>95\%$) for most fault types ($F_1$, $F_2$, $F_4$, $F_5$, $F_7$). The mis-classifications happened mostly on the data in $F_6$ (low air stoichiometry fault) state, in which the cell voltages show vary slightly compared with those in normal state. We also observe that the wrongly diagnosed data are mostly distributed in the initial stage of the fault where the data are located in the transition zone between clear normal state and faulty states.

### 6.2. Online computational complexity

Since the diagnosis approach is implemented using the ASIC whose computing capability and storage capacity are limited compared with a standard PC, the online computational complexity of the algorithm needs to be evaluated. In our approach, the needed memories are respectively $O(ML)$ and $O(LS)$ for saving the trained feature extraction and classification models, in which $S$ is the number of support vectors, while the online computing times are $O(ML)$ and $O(LS)$ for implementing the feature extraction and classification methods. From our test, the occupied memory is less than 200 kb for saving the parameters for diagnosis, while the online implementing time of a diagnosis cycle can be maintained at the level of 10 ms using the developed ASIC. In our platforms, the sample time was set to 1 s, which means the diagnosis cycle can be achieved by a large margin. To our knowledge, the diagnosis cycle obtained in our test could satisfy the requirements for most fuel cell systems.

### 6.3. Novel fault mode recognition

Conventional classification methods can only be used to recognize the known faults which have been shown in the training database. When an example from a new fault mode is treated, it will be diagnosed wrongly into a known fault class or the normal one. We propose here the modified SVM and diagnostic rule to overcome this shortcoming. To verify the proposal, we assumed that a fault is unknown in the training process, and occurs in the diagnosis stage. Taking the case of a 40-cell stack as example, when $F_3$, $F_4$, $F_5$, $F_6$ were considered as the unseen fault, the probabilities that they were successfully recognized as a novel fault mode are respectively 96.77%, 100.00%, 95.36%, 39.86% which are at a high level except the case of $F_6$. This results from the fact that the data in

$F_6$ are too close to the normal ones. They are mostly classified into the normal state class.

### 6.4. Online adaptation

In consideration of the ageing effects, the performance of the PEMFC degrades with time. It results that the variables measured in the normal operating state are non-stationary, i.e. the cell voltages decrease to some degree after a period of time operation. Accordingly, the location of data in normal state varies in the feature space (Fig. 7(d)). In this case, the initially trained diagnosis approach may gradually lose its efficiency, i.e., the FAR increases. To maintain the performance, we propose here an online adaptation method. The online adaptation is realized via incremental learning of the SSM-SVM classifier. We tested the diagnosis approach with and without online adaptation during long-term operation. The 1st, 2nd, and 3rd tests were carried out respectively at three different time points (the 20th day, 80th day, 170th day counting from the beginning of the test). With the initially trained diagnosis model (without online adaptation), the FARs obtained at the 1st, 2nd, and 3rd tests were respectively 35.5%, 100%, and 100%. This means that more and more data in normal state were diagnosed as the faulty ones if we did not modify the initially trained model. By contrast, with our proposed online adaptation method, the FARs obtained at the 1st, 2nd, and 3rd tests were respectively 0.25%, 0%, and 0%. The performance of the diagnosis approach was therefore maintained.

### 6.5. Discussion

The data studied in this paper were acquired from the stacks operated in nominal steady state. In some applications such as fuel cell vehicles, dynamic operating conditions should be handled in diagnosis. In these cases, the correlations of the samples could be considered. To achieve this, data series instead of single data sample could be treated as the objects for classification [39].

Data-driven diagnosis approach is focused on in this study to coordinate with the cell voltage measurement. The proposed approach can be combined with some model-based techniques to handle the system dynamics and to improve the generalization capability. Hybrid diagnosis approach could be one promising solution for fuel cell diagnosis [40].

The proposed data-driven approach is supposed to be applied jointly with the developed ASIC. Although in the current commercial PEMFC systems, it is not easy to measure individual cell voltages. We believe that the proposal can be interesting for many fuel cell suppliers and can be a potential solution in their future products.

## 7. Conclusion

In this study, we firstly propose the criteria for online fuel cell online diagnosis. To attain these criteria, we experimentally demonstrated an online fault diagnosis strategy for PEMFC systems. With the specifically designed ASIC, the proposed diagnosis approach was implemented online to diagnose multiple faults with

respect to several PEMFC stacks. We proposed here to monitor the individual fuel cell voltages and employ them as the variables for diagnosis. In contrast to most of the available approaches in which the fuel cell voltages are assumed to be identical, the inhomogeneity among cells was utilized and dedicated to fault diagnosis. From a fundamental point of view, different faults can cause different thermal, fluidic, electrochemical spatial distributions and these can be reflected by the amplitudes of individual cell voltages. In this study, it was proved that the individual cell voltages possess the discriminative information of different health states. The importance of monitoring every cell voltage, or several of them together, was therefore stressed. From the diagnostic results of online validation, the diagnosis accuracy can be maintained at a high level with respect to different types of fault and for different fuel cell stacks thanks to the utilization of FDA and SVM methods. Besides, the capabilities of recognition an unseen faulty mode and online adaptation, which the traditional diagnosis methods are not capable of handling, were installed into our approach. The efficiency of the ASIC that we designed here, which is dedicated to precisely measuring and online implementing the diagnosis algorithm, was validated. The ASIC therefore promises to be used as a routine component for monitoring fuel cell voltage and implementing the diagnosis approach we proposed here.

Several directions can be interesting on fuel cell diagnosis. First, more general system model should be built in consideration of different faulty conditions. Second, more advanced data-based techniques can be applied to improve the adaptability of the diagnosis methods. Third, the fault diagnosis should be combined with control strategy to improve the fuel cells' reliability finally.

## Acknowledgement

## References

[1] J. Wang, Barriers of scaling-up fuel cells: cost, durability and reliability, Energy 80 (2015) 509–521. https://doi.org/10.1016/j.energy.2014.12.007. http://www.sciencedirect.com/science/article/pii/S0360544214013644.

[2] L. Dubau, L. Castanheira, F. Maillard, M. Chatenet, O. Lottin, G. Maranzana, J. Dillet, A. Lamibrac, J.-C. Perrin, E. Moukheiber, et al., A review of PEM fuel cell durability: materials degradation, local heterogeneities of aging and possible mitigation strategies, Wiley Interdiscip. Rev.: Energy Environ. 3 (6) (2014) 540–560.

[3] R. Borup, J. Meyers, B. Pivovar, Y.S. Kim, R. Mukundan, N. Garland, D. Myers, M. Wilson, F. Garzon, D. Wood, et al., Scientific aspects of polymer electrolyte fuel cell durability and degradation, Chem. Rev. 107 (10) (2007) 3904–3951.

[4] Z. Zheng, R. Petrone, M. Péra, D. Hissel, M. Becherif, C. Pianese, N. Yousfi Steiner, M. Sorrentino, A review on non-model based diagnosis methodologies for PEM fuel cell stacks and systems, Int. J. Hydrogen Energy 38 (21) (2013) 8914–8926, https://doi.org/10.1016/j.ijhydene.2013.04.007. http://linkinghub.elsevier.com/retrieve/pii/S0360319913008550.

[5] G. Tian, S. Wasterlain, I. Endichi, D. Candusso, F. Harel, X. François, M.-C. Péra, D. Hissel, J.-M. Kauffmann, Diagnosis methods dedicated to the localisation of failed cells within PEMFC stacks, J. Power Sources 182 (2) (2008) 449–461. https://doi.org/10.1016/j.jpowsour.2007.12.038. http://www.sciencedirect.com/science/article/pii/S0378775307027061.

[6] R. Petrone, Z. Zheng, D. Hissel, M. Péra, C. Pianese, M. Sorrentino, M. Becherif, N. Yousfi-Steiner, A review on model-based diagnosis methodologies for PEMFCs, Int. J. Hydrogen Energy 38 (17) (2013) 7077–7091. https://doi.org/10.1016/j.ijhydene.2013.03.106.

[7] S.X. Ding, Model-based Fault Diagnosis Techniques, vol. 2013, Springer, 2008.

[8] A. Hernandez, D. Hissel, R. Outbib, Modeling and fault diagnosis of a polymer electrolyte fuel cell using electrical equivalent analysis, IEEE Trans. Energy Convers. 25 (1) (2010) 148–160, https://doi.org/10.1109/TEC.2009.2016121.

[9] S. de Lira, V. Puig, J. Quevedo, A. Husar, LPV observer design for PEM fuel cell system: application to fault detection, J. Power Sources 196 (9) (2011) 4298–4305. https://doi.org/10.1016/j.jpowsour.2010.11.084. http://www.sciencedirect.com/science/article/pii/S0378775310020756.

[10] S. Laghrouche, J. Liu, F. Ahmed, M. Harmouche, M. Wack, Adaptive second-order sliding mode observer-based fault reconstruction for pem fuel cell air-feed system, Contr. Syst. Technol., IEEE Trans. 23 (3) (2015) 1098–1109, https://doi.org/10.1109/TCST.2014.2361869.

[11] T. Escobet, D. Feroldi, S. de Lira, V. Puig, J. Quevedo, J. Riera, M. Serra, Model-based fault diagnosis in PEM fuel cell systems, J. Power Sources 192 (1) (2009) 216–223. https://doi.org/10.1016/j.jpowsour.2008.12.014. http://www.sciencedirect.com/science/article/pii/S0378775308023288.

[12] S. Yin, Data-driven Design of Fault Diagnosis Systems, Ph.D. thesis, Universität Duisburg-Essen, Fakultät für Ingenieurwissenschaften>> Ingenieurwissenschaften-Campus Duisburg>> Abteilung Elektrotechnik und Informationstechnik>> Automatisierung und komplexe Systeme, 2012.

[13] D. Hissel, D. Candusso, F. Harel, Fuzzy-clustering durability diagnosis of polymer electrolyte fuel cells dedicated to transportation applications, IEEE Trans. Veh. Technol. 56 (5) (2007) 2414–2420.

[14] Z. Li, R. Outbib, S. Giurgea, D. Hissel, Diagnosis for pemfc systems: a data-driven approach with the capabilities of online adaptation and novel fault detection, Ind. Electr. IEEE Trans. 62 (8) (2015) 5164–5174, https://doi.org/10.1109/TIE.2015.2418324.

[15] D. Hissel, M.C. Péra, J.M. Kauffmann, Diagnosis of automotive fuel cell power generators, J. Power Sources 128 (2) (2004) 239–246. https://doi.org/10.1016/j.jpowsour.2003.10.001.

[16] N. Yousfi-Steiner, D. Hissel, P. Moçotéguy, D. Candusso, Diagnosis of polymer electrolyte fuel cells failure modes (flooding & drying out) by neural networks modeling, Int. J. Hydrogen Energy 36 (4) (2011) 3067–3075. https://doi.org/10.1016/j.ijhydene.2010.10.077.

[17] Y. Vural, D.B. Ingham, M. Pourkashanian, Performance prediction of a proton exchange membrane fuel cell using the ANFIS model, Int. J. Hydrogen Energy 34 (22) (2009) 9181–9187, https://doi.org/10.1016/j.ijhydene.2009.08.096.

[18] J. Hua, J. Li, M. Ouyang, L. Lu, L. Xu, Proton exchange membrane fuel cell system diagnosis based on the multivariate statistical method, Int. J. Hydrogen Energy (2011) 1–10. https://doi.org/10.1016/j.ijhydene.2011.05.075.

[19] Z. Zheng, M.-C. Péra, D. Hissel, M. Becherif, K.-S. Agbli, Y. Li, A double-fuzzy diagnostic methodology dedicated to online fault diagnosis of proton exchange membrane fuel cell stacks, J. Power Sources 271 (2014) 570–581. https://doi.org/10.1016/j.jpowsour.2014.07.157. http://www.sciencedirect.com/science/article/pii/S0378775314012117.

[20] L. Alberto, M. Riascos, M.G. Simoes, P.E. Miyagi, On-line fault diagnostic system for proton exchange membrane fuel cells, J. Power Sources 175 (2008) 419–429.

[21] S. Wasterlain, D. Candusso, F. Harel, X. François, D. Hissel, Diagnosis of a fuel cell stack using electrochemical impedance spectroscopy and bayesian networks, in: Vehicle Power and Propulsion Conference (VPPC), 2010, IEEE, 2010, pp. 1–6, https://doi.org/10.1109/VPPC.2010.5729184.

[22] J. Chen, B. Zhou, Diagnosis of PEM fuel cell stack dynamic behaviors, J. Power Sources 177 (1) (2008) 83–95. https://doi.org/10.1016/j.jpowsour.2007.11.038.

[23] N.Y. Steiner, D. Hissel, P. Moçotéguy, D. Candusso, Non intrusive diagnosis of polymer electrolyte fuel cells by wavelet packet transform, Int. J. Hydrogen Energy 36 (1) (2011) 740–746. https://doi.org/10.1016/j.ijhydene.2010.10.033. http://www.sciencedirect.com/science/article/pii/S0360319910021129.

[24] D. Benouioua, D. Candusso, F. Harel, L. Oukhellou, Fuel cell diagnosis method based on multifractal analysis of stack voltage signal, Int. J. Hydrogen Energy 39 (5) (2014) 2236–2245. https://doi.org/10.1016/j.ijhydene.2013.11.066. http://www.sciencedirect.com/science/article/pii/S0360319913027912.

[25] E. Monmasson, M. Cirstea, FPGA design methodology for industrial control systems—A review, Ind. Electr. IEEE Trans. 54 (4) (2007) 1824–1842, https://doi.org/10.1109/TIE.2007.898281.

[26] C. Steiger, H. Walder, M. Platzner, Operating systems for reconfigurable embedded platforms: online scheduling of real-time tasks, Comput. IEEE Trans. 53 (11) (2004) 1393–1407, https://doi.org/10.1109/TC.2004.99.

[27] P. Rodatz, F. Büchi, C. Onder, L. Guzzella, Operational aspects of a large PEFC stack under practical conditions, J. Power Sources 128 (2) (2004) 208–217. https://doi.org/10.1016/j.jpowsour.2003.09.060. http://www.sciencedirect.com/science/article/pii/S0378775303010085.

[28] Z. Li, R. Outbib, S. Giurgea, D. Hissel, Y. Li, Fault detection and isolation for polymer electrolyte membrane fuel cell systems by analyzing cell voltage generated space, Appl. Energy 148 (2015) 260–272. https://doi.org/10.1016/j.apenergy.2015.03.076. http://www.sciencedirect.com/science/article/pii/S0306261915003682.

[29] E. Gerstner, Nobel prize 2007: Fert and grünberg, Nat. Phys. 3 (11) (2007) 754.

[30] Y. S. Chai, S. Kwon, S. H. Chun, I. Kim, B.-G. Jeon, K. H. Kim, S. Lee, Electrical control of large magnetization reversal in a helimagnet, Nat. Commun. 5.

[31] Z. Li, R. Outbib, D. Hissel, S. Giurgea, Data-driven diagnosis of PEM fuel cell: a comparative study, Contr. Eng. Pract. 28 (2014) 1–12, https://doi.org/10.1016/j.conengprac.2014.02.019. http://linkinghub.elsevier.com/retrieve/pii/S0967066114001002.

[32] G. McLachlan, Discriminant Analysis and Statistical Pattern Recognition, vol. 544, John Wiley & Sons, 2004.

[33] J.C. Platt, Sequential Minimal Optimization : a Fast Algorithm for Training Support Vector Machines, Technical Report MSR-TR-98-14, Microsoft Research, 1998, pp. 1–21.

[34] P.Y. Hao, Y.H. Lin, A new multi-class support vector machine with multi-sphere in the feature space, in: Proceedings of the 20th International Conference on Industrial, Engineering, and Other Applications of Applied Intelligent Systems, IEA/AIE'07, Springer-Verlag, Berlin, Heidelberg, 2007, pp. 756–765.

[35] P. Freitas, R. Ferreira, S. Cardoso, F. Cardoso, Magnetoresistive sensors, J. Phys. Condens. Matter 19 (16) (2007), 165221.

[36] M. Pannetier-Lecoeur, C. Fermon, A. Giraud, GMR based integrated non-contact voltage sensor for fuel cells monitoring, in: Sensing Technology (ICST), 2011 Fifth International Conference on, 2011, pp. 101—105, https://doi.org/10.1109/ICSensT.2011.6136941.

[37] Z. Li, S. Giurgea, R. Outbib, D. Hissel, Online diagnosis of PEMFC by combining support vector machine and fluidic model, Fuel Cell. 14 (3) (2014) 448—456. http://doi.wiley.com/10.1002/fuce.201300197.

[38] C. de Beer, P.S. Barendse, P. Pillay, Fuel cell condition monitoring using opti-mized broadband impedance spectroscopy, IEEE Trans. Ind. Electron. 62 (8) (2015) 5306—5316, https://doi.org/10.1109/TIE.2015.2418313.

[39] Z. Li, R. Outbib, S. Giurgea, D. Hissel, Fault diagnosis for pemfc systems in consideration of dynamic behaviors and spatial inhomogeneity, IEEE Trans. Energy Convers. (2018) 1, https://doi.org/10.1109/TEC.2018.2824902.

[40] Z. Li, R. Outbib, D. Hissel, S. Giurgea, Diagnosis of pemfc by using data-driven parity space strategy, in: 2014 European Control Conference (ECC), 2014, pp. 1268—1273, https://doi.org/10.1109/ECC.2014.6862527.